Experimental constraints on magnetic stability of chondrules and the paleomagnetic significance of dusty olivines

Minoru Uehara *, Norihiro Nakamura

Department of Geo-Environmental Sciences, Tohoku University, Sendai, Miyagi 980-8578, Japan

Abstract

Dynamic crystallization experiments are conducted under a magnetic field to determine both magnetic and mineralogical properties of chondrules. The experiment reproduced synthetic dusty olivine samples that were formed by a high temperature reduction of an initially fayalitic olivine. Backscattered-electron microscopy observations confirmed that synthetic dusty olivine contains abundant fine, submicron-sized Ni-poor Fe inclusions in the cores of MgO-rich olivine grains, similar to that in natural chondrules. Alternating field demagnetization experiments of dusty olivine samples indicate mean destructive fields of up to 80 mT, suggesting the submicron-sized Fe inclusions are a carrier of stable remanence. In natural chondrules, fine Fe inclusions in the dusty olivine may have been armored against chemical alteration by surrounding host olivine crystals. Since the fine Fe inclusions were probably heated above the Curie temperature during the last chondrule forming events, the fine Fe inclusions in dusty olivine can acquire thermal remanent magnetization during the chondrule formation event. Theoretical time–temperature relation of such fine-grained Fe (kamacite) grains suggested that a paleomagnetic data observed above 490 °C in thermal demagnetization experiments of dusty olivines is reliable despite the low-grade metamorphism of unequilibrated ordinary chondrites (e.g., LL3.0). Therefore, the presence of fine Fe inclusions in dusty olivine in unequilibrated ordinary chondrites constrains that such dusty olivine in chondrules is a good candidate as an un-altered and stable magnetic recorder of the early solar magnetic field.
© 2006 Elsevier B.V. All rights reserved.

1. Introduction

Chondrules are millimeter to submillimeter-sized spherical materials mainly composed of olivine, pyroxene, glassy mesostasis and metals. Some metals are of ferromagnetic and carry a remanent magnetization. Chondrules comprise the dominant fraction of most chondritic meteorites and are the products of partial melting of aggregates of fine-grained silicates with minor contributions from metals, sulfides and oxides [1]. It is generally accepted that chondrules were formed by flash melting events: the precursor dust aggregates were heated to high temperature and cooled back down in several minutes [2–4]. Previous dynamic crystallization experiments showed that the degree of melting controls internal textures of synthetic chondrules [5] and reduction reactions produce many mineralogical features characteristic of natural unequilibrated chondrules, such as relict dusty olivine grains [5–11]. Therefore, the internal textures of chondrules provide an indicator of thermal

* Corresponding author. Tel.: +81 22 795 6613; fax: +81 22 795 6634.
  E-mail address: syok@dges.tohoku.ac.jp (M. Uehara).

and chemical environments during chondrule formation [5]. Individual chondrules are expected to have acquired a thermal remanent magnetization (TRM) when magnetic minerals cooled below their Curie point temperatures. Thus, a natural remanent magnetization (NRM) of an individual chondrule gives evidence for the presence of an extraterrestrial magnetic field in the early solar nebula, providing quantitative information for a magnetic field-driven bipolar outflow of the protoplanetary disk [12]. However, even in low petrologic type-3 ordinary or carbonaceous chondrites, chondrules have suffered from thermal and chemical alterations during the long history of the solar system mostly early on first < 100 My. These alteration processes may re-magnetize primary remanence, and this may result in misleading interpretations of the timing of remanence and the paleofield intensity in the early solar nebula. Nevertheless, a paleointensity of 0.07 to 0.7 mT estimated from individual chondrules of the Allende (CV3) chondrite [13,14] has provided a fundamental constraint for astrophysical simulation studies for the early evolution of the solar nebula [12,15,16].

In order for chondrules to maintain a record of the intensity of a nebula's magnetic field over billions of years, their remanence must be stable in the face of variations in temperature and chemical environment, and redox state caused by common parent-body or terrestrial geologic processes such as metamorphism, weathering and hydrothermal alteration. It is believed that typically used magnetic recorders, such as chondrules in the Allende (CV3) carbonaceous chondrite, have successfully preserve the record of the nebula's magnetic field, because NRM of individual chondrules is reasonably stable and coherent against alternating field (AF) demagnetization [13,17]. Iron–Nickel (Fe–Ni) metals are major magnetic minerals in primitive ordinary chondrites [18,19]. Although Fe–Ni metals show various shape and size, they are generally coarse (20–150 μm) and spheroidal inclusions within a host chondrule [20]. However, Sugiura and Strangway [21] suggested that coarse, > 100 μm sized, Fe–Ni grains have acquired an isothermal remanence through the exposure to an artificial magnet by investigators. This is because coarse-grained metals possess numerous magnetic domain walls that easily rearrange their spin configurations even in weak external field, resulting in the destruction of primary remanence. On the other hand, fine-grained metals with few domain walls are capable of carrying stable remanence due to their high coercivity (e.g., [22]). To survive artificial magnetic exposure and terrestrial field reversal, a highly coercive fine-grained mineral is needed for paleomagnetic studies of chondrules. Previous researchers proposed tetrataenite as an alternative candidate, because tetrataenite shows high

coercivity due to an ordered crystal of 50% Fe–50% Ni in atomic ratio [23]. However, tetrataenite acquired an external magnetic field during a low-temperature atomic ordering process of transformation from disordered taenite to ordered tetrataenite [23]. Therefore, the NRM of tetrataenite appears to be a transformation remanence from parent-body metamorphism, rather than a primary remanence during the nebular thermal process. Thus, in order to understand magnetic fields in the solar nebula, we need to explore which minerals are the least altered and most stable magnetic recorders for the early solar magnetic field.

Fine-grained Fe inclusions hosted in Mg-rich olivines ("dusty olivines") of unequilibrated chondrites may be an alternative medium to study the solar nebula magnetic fields [6,7,10,20,24,25]. Dusty olivine grains are commonly preserved in chondrules of unequilibrated chondrites. In unequilibrated ordinary chondrites, dusty olivine chondrule occurs in about 10% of all chondrules [26]. The fine-grained Fe inclusions in dusty olivine are submicron in size, and are often aligned along crystallographic directions of host forsteritic olivine grains [10,20,25]. The chemical composition is low-nickel metallic Fe (>99 wt.% Fe) [24,25], and the dusty iron core is commonly surrounded by clear olivine rim that has a composition similar to the normal grains of the host chondrules [10,20,24,25]. The olivine host isolates the submicron iron inclusions against chemical alteration by hydrothermal fluids and protects the dusty olivine from terrestrial and extraterrestrial oxidation. Although these grains may be resistive to magnetic field variations, it is uncertain whether a primary remanence had survived under an asteroidal metamorphic process and have been retained for a long time.

Néel's [27] single-domain thermal activation theory represents that the thermal relaxation time (τ) of single-domain magnetized grains can be expressed as [22,28]:

$$\tau = \frac{1}{C} \exp\left[\frac{v h_c j_s \beta^n(T)}{2kT}\right] \qquad (1)$$

where C is a frequency factor (10^{8-10} s^{-1}), v is the grain's volume, h_c is microscopic coercivity, $\beta^n(T)$ is normalized T dependence of saturation magnetization j_s [29], n depends on the mechanism of anisotropy, k is Boltzmann's constant, and T is temperature [30]. The fundamental implication is that the grain moments will relax in a short time when the available thermal energy is comparable to magnetic energy barriers ($v h_c j_s \beta^n(T)$) opposing reversal of grain moments, but a very long time otherwise. Because τ depends exponentially on T and $j_s \beta^n(T)$, grains with a particular v and h_c will acquire a permanent NRM when they are cooled a few °C through their blocking temperature T_B, at which $\tau \approx t$, a typical

laboratory thermal demagnetization time. The NRM of the same grains will be thermally demagnetized when reheated through the unblocking temperature T_{UB}, at which τ is again $\approx t$. Since Fe inclusions in dusty olivine are uniform assemblages of submicron-sized body centered cubic (bcc) grains, the relaxation time continues to increase exponentially during cooling and the acquired TRM can be retained over billions of years. Terrestrial analogs of fine-grained magnetic carriers include submicron-sized inclusions of magnetite and titanomagnetite that have been observed in pyroxene and plagioclase in mafic intrusive rocks [31–37], and magnetite inclusions in the basaltic glass of ocean-floor basalts [38]. These submicron-sized magnetite inclusions have successfully preserved and recorded ancient geodynamo behavior even though they have suffered a terrestrial alteration [39]. Therefore, the submicron-sized Fe inclusions in dusty olivine are expected to be excellent candidates for paleomagnetic studies of the early solar nebula. Previous studies have confirmed that the dusty olivine texture can be synthesized in reducing conditions by adding graphite or diamond into precursory silicate dust [8,9,25]. However, there have been few experimental determinations for both magnetic and mineralogical properties of dusty olivine chondrule through dynamic crystallization experiments under magnetic field. To explore the issues of the magnetic stabilities of dusty olivines, we conducted high-temperature reduction experiments under magnetic field and constrained magnetic stabilities of natural chondrules from the experiment of reduced olivines.

2. Method

The starting material is powdered olivines collected from mantle rock xenolith of the Ichinomegata volcanic crater, NE Japan [40]. Back-scattered electron (BSE) imaging, element X-ray intensity maps, and quantitative analyses were performed on a JEOL-5800LV, equipped with an energy dispersive spectrometer (EDS) (Model 6841, Oxford Instruments) and operating at 15 kV and 30 nA. Modal proportions of minerals in the starting material based on X-ray intensity maps were 93.9 vol.% olivine, 5.5 vol.% diopsite, and 0.6 vol.% spinel. Representative mineral compositions and calculated bulk composition are listed in Table 1. The composition of the olivine is determined as Mg-rich olivine $(Mg_{0.9}Fe_{0.1})_2SiO_4$ with trace amount of Al, Mn, and Ni, diopside with small amounts of Al, and Cr-rich spinel. This fayalitic composition of the olivine (Fa_{10}) is a good proxy of relict dusty olivine grains in natural chondrules of unequilibrated chondrites because the composition is close to the composition of natural dusty olivines prior to reduction [10]. The olivine sample was firstly crushed by stainless steel bowl

Table 1
Representative compositions of the minerals in the starting materials (data in wt.%)

	Olivine	Diopsite	Spinel	Bulk [a]
SiO_2	41.5±0.5	54.9±0.8	n.d.	44.8
Cr_2O_3	n.d.	1.0±0.3	31.2±0.4	0.25
Al_2O_3	0.5±0.1	4.5±0.5	37.4±0.4	0.91
FeO	9.8±0.6	2.8±0.2	14.5±0.2	9.0
MnO	0.2±0.1	n.d	n.d	0.14
MgO	48.4±0.8	17.3±0.4	18.1±0.2	43.7
CaO	n.d	20.1±0.9	n.d.	1.2
NiO	0.5±0.1	n.d	n.d.	0.43
Na_2O	n.d	0.9±0.3	n.d.	0.05
Total	100.8±0.9	101.5±0.4	101.3±0.8	100.1
Fa (mol%)	10.2±0.7			

All compositions are means of five EDS analyses.
n.d.=not detected.
[a] Bulk composition of the starting material calculated from the modal abundances and representative compositions of the minerals.

and milled by an automatic agate mortar into 5–50 µm (average 23 µm), and was not sieved. Approximately 10–50 mg of the starting material was used to produce synthetic chondrules. The grain size distribution was small enough to completely melt in short duration (seconds to minutes) and to produce a variety of textures including barred olivine chondrules [5,41]. In 2 of 13 experiments we added 3 mg of carbon in the form of graphite powder into starting materials. A vacuumed quartz glass tube furnace was hand-made to simulate chondrule formation through a flash-heating regime under a magnetic field (Fig. 1). In the quartz tube, stainless steel electrodes supported a heating wire loop which was made from tungsten wire (ϕ 0.4 mm) with looped eight times. The load voltage was from 0 to 12 V, and the load current was from 0 to 10 A. A hand-made graphite crucible (3.5 and 5 mm in inner and outer diameters, respectively, 10 mm in height and 9 mm in depth) was settled in the center of the heating wire loops, and its bottom was supported by an alumina tube on a graphite base plate. Glass fiber thermowool was stuffed to insulate the crucible from the heating wire loops and tungsten vapors. We used a Tungsten–Rhenium alloy thermocouple (W95%Re5%–W74% Re26%) placed just below the sample to monitor temperature. The thermocouple was calibrated against the melting point of copper (m.p.=1084.5 °C). The glass tube was evacuated to 10 Pa by an oil rotary vacuum pump. The output signal of the thermocouple was amplified and recorded onto the computer by an analog to digital converter (ADC). The gain of the amplifier was 100 and the resolution of the ADC was 12-bit, which assures a resolution of 1 °C. The furnace temperature was controlled by manual adjustment of the load current. To achieve a stable heating and cooling, we used monitoring
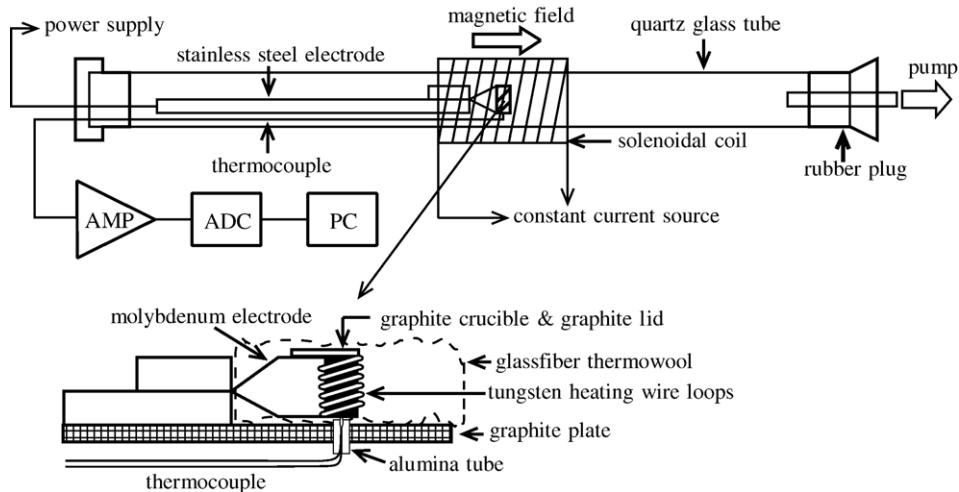
Fig. 1. Schematic illustration of the quartz glass tube furnace attached with a magnetic field generation coil.

software that draws both a measured–temperature curve and an ideal linear heating–cooling profile. The heating sequences were programmed as follows: the crucible was heated to the peak temperature (about 1350 °C), held that for 200 to 600 s, and cooled at 1000 °C/h to 8000 °C/h down to the Curie temperature of Fe–Ni metal (750 °C), then quenched.

In order to explore the effect of chondrule textures on magnetic acquisition during cooling, a solenoidal coil was settled around the furnace, driving the intensity of an applied field of 1–12 mT. A constant current source supplied a stabilized current to the coil, producing a noiseless DC magnetic field. To avoid a magnetic field induced by the current of the heating wire coil, we cut off the power supply for the heating wire loops above 750 °C which corresponds to the Curie temperature of Fe–Ni metal. Note that this applied field is much stronger than the paleosolar magnetic field estimated from carbonaceous chondrites as 0.07–0.7 mT [13,14]. We marked the direction of an applied magnetic field on the synthetic chondrule samples within 5° orientation variations. The remanent magnetization of the samples was measured using a spinner magnetometer (minispin, Molspin Inc.). A stepwise alternating field (AF) demagnetization procedure was performed by the minispin and a three-axis tumbling AF demagnetizer (DEM 95, Natsuhara Giken Inc.). The maximum alternating field was set on 160 mT. For weak intensity samples, we used a superconducting

Table 2
Experimental conditions, textures and magnetic properties

	Texture	Peak temperature (°C)	Duration time [a] (s)	Cooling rate (°C/h)	Applied field (mT)	RM [b] (10^{-3} A m^2/kg)
Dusty-0	Dusty	1334	597	2900	12	1.18
Dusty-1	Dusty	1300	435	– [c]	9	3.38
Dusty-2	Dusty	1310	309	3780	12	16.3
Dusty-4	Dusty	1306	205	6315	12	5.50
Dusty-5	Dusty	1065	0	– [c]	– [d]	–
Dusty-6	Dusty	1335	241	3813	12	4.47
Dusty-7 [e]	Dusty	1381	262	2350	1	4.55
Dusty-8 [e]	Dusty	1388	225	2390	1	0.901
BO-1	BO	1333	369	1290	12	0.0130
BO-2	BO	1350	187	7566	12	–
PO-0	PO	1350	269	2500	– [d]	0.0574
PO-1	PO	1190	140	– [c]	1	3.88

[a] Duration time at peak temperature.
[b] RM=remanent magnetization.
[c] Quenched from a peak temperature.
[d] Geomagnetic field.
[e] Added graphite in the starting materials.

quantum interference device (SQUID)-magnetometer with online AF demagnetizer (Model 755R, 2G Enterprise) at National Institute of Polar Research (NIPR). The maximum alternating field of the NIPR SQUID magnetometer system was set on 100 mT. AF demagnetization proceeded until the intensities fall below the detection limit of the magnetometer. A high-temperature thermomagnetic curve was measured under a strong field (1 T) in 10^{-4} Pa atmospheric pressure using a vibrating sample magnetometer (Riken Denshi Co., Ltd.) at NIPR. During the vibration measurements, a chipped sample was heated from room temperature to 780 °C with heating and

cooling rates of 375 °C/h. Since the measured intensity changing of the 1 T magnetization approximated sample's saturated remanence at high temperature, the sample's Curie temperature was determined as the points of major decrease in high-temperature thermomagnetic curve.

3. Rock magnetic and electron microscope analyses

All the run products become magnetized when the magnetic minerals were cooled through their Curie temperature under the applied magnetic field. The intensity of initial remanent magnetization of each sample and
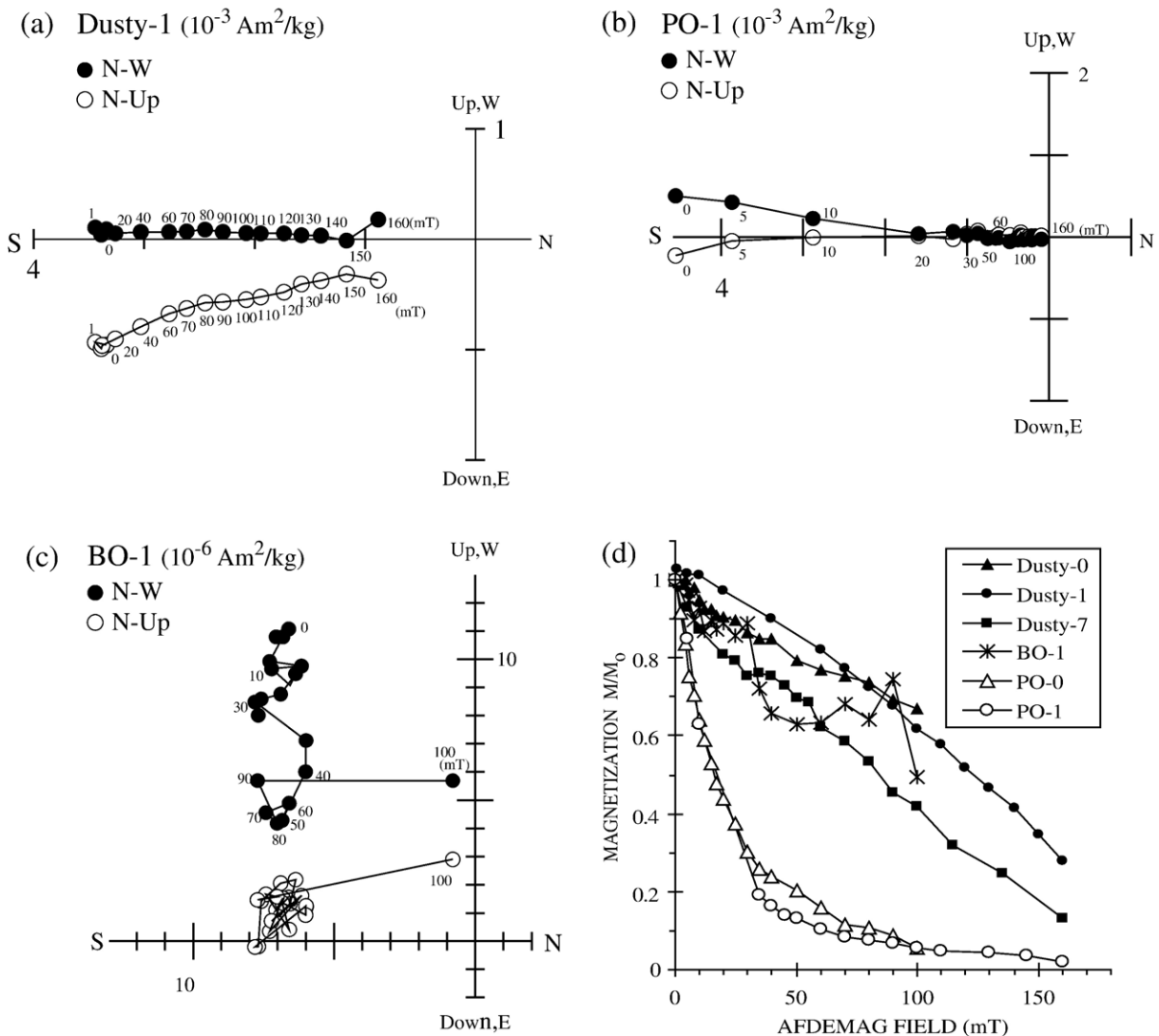

Fig. 2. (a, b, c) Representative orthogonal vector plots of alternating field (AF) demagnetization data of dusty olivine texture (Dusty-1), porphyritic olivine texture (PO-1), and barred olivine texture (BO-1). Numbers correspond to demagnetization field intensities. (d) Normalized AF demagnetization curves of remanent magnetizations for synthetic chondrules. Remanence of dusty olivine texture contains a high coercivity component, and shows more stable behavior than that of porphyritic olivine texture. Barred olivine texture shows very unstable behavior.

experimental conditions are listed in Table 2. Fig. 2 represents demagnetization data on orthogonal vector component diagrams of representative samples. Because we applied a strong northward magnetic field, data points in our vector component diagrams are expected to show a trajectory toward the origin with no significant change in direction. Fig. 2 also shows normalized AF demagnetization curves. The field required to destroy one half the remanence is called the mean destructive field, and serves as a proxy for the sample's coercivity. The results of AF demagnetization characterize the samples into three distinct groups.

The samples reacted with carbon crucibles (Dusty-0– Dusty-6) and the samples with added carbon (Dusty-7, Dusty-8) hold a strong remanence in the range from 9.01×10^{-4} A m^2/kg to 1.63×10^{-2} A m^2/kg, and they are extremely stable against AF demagnetization following a weakly sigmoid-shaped curve. A representative vector component diagram of the Dusty sample presents a high coercivity component (20–160 mT) that was not completely demagnetized up to peak fields of 160 mT (Fig. 2a). Normalized AF demagnetization curves indicate that the remaining intensity of remanence ranges from 15% to 30% of the initial intensities after demagnetization at 160 mT (Fig. 2d). The mean destructive field of Dusty samples exceeds 80 mT. Fig. 3 shows a high temperature thermomagnetic curve of Dusty-4. The result indicates a clear Curie point at 760 °C with a reversible cooling path, corresponding to that of Fe–Ni alloy of low-Ni (<7 wt.%) kamacite [18,19].

The PO-0 and PO-1 samples with no carbon added hold moderate remanences in the range of 5.74×10^{-5} A m^2/kg
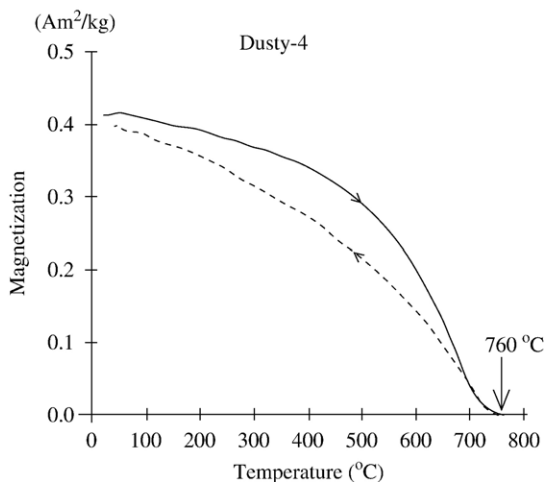

Fig. 3. Thermomagnetic curve of synthetic dusty olivine, obtained by a vibrating sample magnetometer at NIPR. A chipped sample was heated to 780 °C under 1 T magnetic field in 10^{-4} Pa vacuumed condition. The heating line (solid line) and cooling line (dashed line) are reversible.

and 3.88×10^{-3} A m^2/kg. Although the PO samples contain a high coercivity component, a vector component diagram indicates that a low coercivity component (0–25 mT) is dominant in PO samples, being different from Dusty samples (Fig. 2b). The AF demagnetization curves for PO samples show intermediately stable behavior following a quasi-exponential curve (Fig. 2d). Their intensities decay steeply to compare with stable Dusty samples. The mean destructive field of PO samples is about 20 mT.

Sample BO-1 with no carbon added possesses very weak remanence of 1.30×10^{-5} A m^2/kg, even when it has been exposed under a strong magnetic field. Because the AF demagnetization curve for BO-1 is very unstable, we cannot decide the mean destructive field (Fig. 2d). Unlike in the case of the other samples, a vector component diagram shows an erratic pattern (Fig. 2c), indicating that there is no characteristic component in the BO sample.

Fig. 4 shows BSE images of the three typical textures of our synthetic chondrules. The comparison of remanence stabilities with their textures indicates the correlation between textures and magnetic stabilities. Previous studies of natural dusty olivines showed a high density of fine metal inclusions that often aligned along crystallographic directions in host olivine crystals with rims of clear Mg-rich olivine [6,10,20,24,25]. Samples from Dusty-0 to Dusty-8, which show extremely stable remanence, were formed by a reduced condition in the presence of graphite during heating experiments. The Dusty samples contain olivine phenocrysts, glassy mesostasis, and numerous metallic Fe–Ni grains located within or outside olivine crystals (Fig. 4a,b). Our BSE observations confirm that the Fe–Ni metal is present as fine (<1 μm) inclusions embedded in olivine, mimicking natural dusty olivines, and as coarse (1–20 μm) Fe–Ni globules located in the glassy mesostasis at the olivine grain boundaries. Occasionally, the fine Fe inclusions in the synthetic dusty olivines occur as linear arrays within a host olivine (Fig. 4b). Our EDS analyses show that clear olivine crystals surrounding the dusty core are more forsteritic (Fa$_{0.5}$–Fa$_{4.6}$) than initial composition (Fa$_{10}$). These features have been observed in natural dusty olivines in chondrules of primitive chondrites, e.g. Murchison (CM2), Bishunpur (LL3.1) and Semarkona (LL3.0) [6,7,10,20,24,25], and have also been observed in synthetic dusty olivines [8,9,25,42,43]. Although the fine Fe inclusions within the olivine crystals are generally too fine-grained to determine the Ni content, a grain in Dusty-6 was large (3 μm) enough to allow a quantitative analysis. EDS analysis confirmed that the grain contains 5 wt.% of Ni, which is comparable the result of Curie
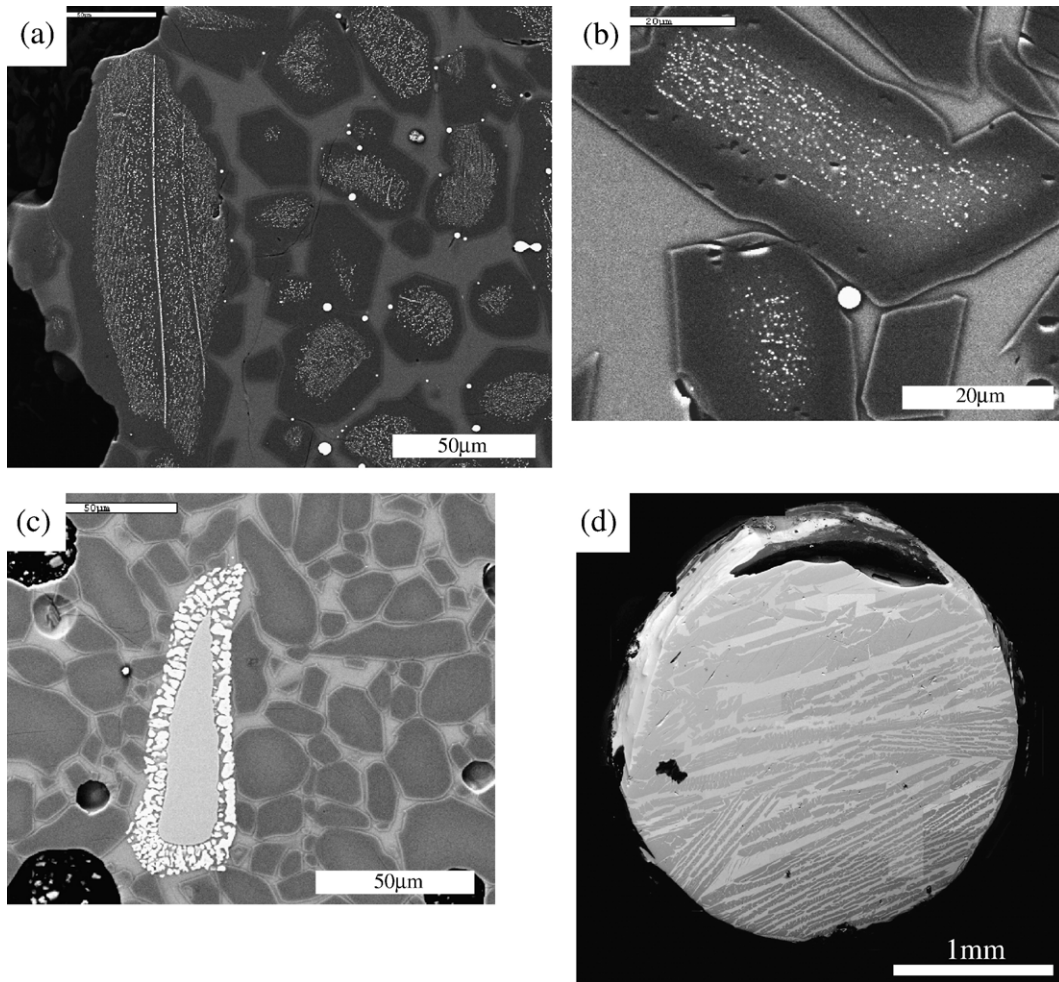
Fig. 4. Backscattered electron images of synthetic chondrules showing typical textures. (a) Dusty-7 shows dusty olivine texture consisting of olivine (dark gray) and abundant metallic phases (white) with Ca, Al-rich glassy mesostasis (light gray). (b) A close up image of dusty olivines in section of Dusty-1. Metallic phases are present as submicron-sized (<1 µm) inclusions within olivine grains and as micron-sized (1 to 50 µm) metal globules embedded in the matrix. Submicron-sized metal inclusions show preferential alignments along the crystallographic direction of the olivine host. (c) Porphyritic olivine texture of PO-1, consisting of olivine (dark gray) and glassy mesostasis (light gray). Metal aggregate contain a large Cr–Al-rich grain (gray) decorated with small Cr-rich particles (white). (d) Barred olivine texture of BO-1. It consists of olivine (dark gray) with glassy mesostasis (light gray).

point measurement. Although the most of olivine crystals in the Dusty samples are "dusty", a portion of olivine crystals in Dusty-0 and Dusty-1 are "clear" that contain no fine Fe inclusions. At the "dusty" olivine grain boundaries, the average Ni content of coarse Fe–Ni globules located in the glassy mesostasis obtained by EDS analyses is 4 wt.% (32 analyses). On the other hand, the average Ni contents of the metal globules located at the "clear" olivine grain boundaries is 41 wt.% (16 analyses). The appearance of the "dusty olivine" and the difference of the composition of the coarse Fe–Ni globules probably reflected local variations in temperature, oxygen fugacity, and/or variability in the initial olivine composition before reduction.

Synthetic dusty olivines in the samples were formed when the olivines were reduced by graphite at high temperature. Samples Dusty-7 and Dusty-8 were reduced by added graphite powder, whereas the other samples from Dusty-0 to Dusty-6 were reduced by the graphite crucibles. Sample Dusty-5 jumped out of the graphite crucible and stuck at its edge, suggesting a production of gas. Except for quenched experiments (Dusty-1, Dusty-5), dusty olivine samples were formed by heating at around 1306 °C–1388 °C for several minutes and cooling at 2390 °C/h–6315 °C/h. The timescales of heating are comparable with results of previous high-temperature reduction experiments that reproduced dusty olivines [8,9,25].

On the other hand, samples BO-1, BO-2, PO-0 and PO-1 were formed under carbon-free experiments. They were not reacted by the graphite crucibles, and their olivine crystals are not "dusty". BSE images show that BO-1 and BO-2 contain multiple olivine plates set in a glassy mesostasis and form in a triangle arrangement (Fig. 4c), similar to a barred olivine texture in natural chondrules [44]. We found no metallic phase in an arbitrary thin section cutting of the barred olivine textured samples, even though it has a very weak remanence. In conjunction with the unstable direction changing during the AF demagnetization, the observed remanence was spurious one probably due to the weak intensity that is below the detection limit of the SQUID magnetometer. Therefore, we suggest that the barred olivine sample may have no useful primary magnetic information.

PO-0 and PO-1 show porphyritic olivine texture that contains sub-rounded olivine phenocrysts whose fayalitic composition is same as initial composition (Fa_{10}), glassy mesostasis, and coarse (15–50 μm) spinel grains surrounded by small (5–10 μm) Fe-bearing Cr–Al metals (Fig. 4d). Although the composition of metal in porphyritic olivine sample are different from that in natural chondrules, their olivine textures resemble to those of natural porphyritic olivine chondrules [44]. These porphyritic texture samples contain coarse-grained metals,

showing similar demagnetization behaviour with very different remanence intensities. This difference depends on the total volume of remanence-carrying coarse-grained metals produced in synthetic chondrules. The larger volume shows the higher intensity in low coercivity range due to the preferred alignment of magnetic domain walls under strong magnetic field. Therefore, the low coercive coarse-grained metals may not retain the primary remanence under an artificial magnet exposure or terrestrial field reversal.

Barred olivine and porphyritic olivine textures were formed by heating at peak temperature of around 1350 °C for 3–6 min and liner cooling at 1290 °C/h–7566 °C/h (Table 2). One quenched experiment also formed a porphyritic olivine texture (PO-1). These thermal conditions are similar to those that produced dusty olivine in our samples. Since oxygen fugacity in the furnace was not fixed by buffering gases (e.g. pure CO gas), factors that controlled oxygen fugacity in the furnace were residual air (∼ 10 Pa) and graphite. Thus, a balance between these two factors could result in the occurrence of Fe metal in our samples. If 20% of the gas in the furnace was oxygen, the oxygen fugacity at 1400 °C is ∼ 2 Pa, being higher than that of iron-wüstite buffer (10^{-15} Pa) [45]. This oxygen fugacity suggests that no metallic Fe would be formed. On the other hand,
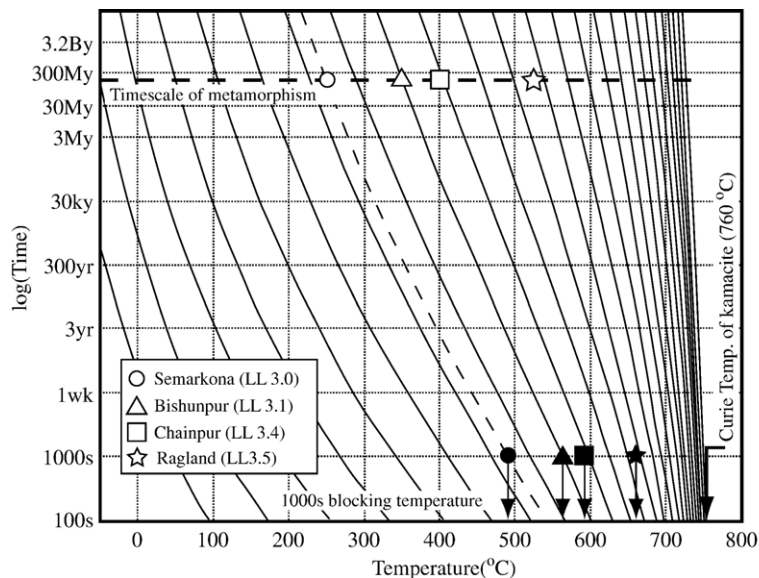

Fig. 5. Time–temperature contour diagram for a particular ensemble of single domain kamacite ($Fe_{1-x}Ni_x$ for $x \leq 0.10$) from Garrick-Bethell and Weiss [47]. The curves are "blocking contours" which trace the possible combinations of blocking temperature and relaxation time, or of reheating temperature and duration time of reheating for which overprinting is just possible. The contours represent the different time–temperature conditions under which a single-domain grain is just on the point of being remagnetized by laboratory reheating. Open symbols are maximum metamorphic temperatures and their duration time (c.a., 100 My) of typical ordinary chondrites including dusty olivines (see Table 3). Solid symbols are 1000 s laboratory unblocking temperatures that would indicate survival potential of primary NRM for each metamorphic grade. Metamorphic temperature estimates are based on Alexander et al. [51] for Semarkona, Rambaldi and Wasson [20] for Bishunpur, Huss and Lewis [35] and Sears et al. [55] for Chainpur and Ragland.

the graphite crucible acts as a reducing agent that maintained oxygen fugacity around the contact area between the olivine melt and the crucible. Although we cannot decide the trigger of the reduction reaction in our experiments, the absence of Fe in the PO and BO samples might be explained by bad wetting between the melted sample and graphite crucible.

4. Time–temperature relations for the re-magnetization by metamorphism

Meteorites of paleomagnetic interest may suffer intervals of heating, possibly resulting in metamorphism. A fundamental survival test is that the reheating temperature should not exceed the lowest blocking temperature used in paleomagnetic studies and also paleofield determination. However, a long reheating duration produces a secondary remanence, which cannot be demagnetized at metamorphic temperature for timescale of laboratory heating (ca. 1000 s). Thus, we must understand how prolonged exposure to elevated temperatures below the Curie temperature will affect the ability of dusty olivines to retain a primary NRM. The Néel's relaxation theory explains how portions of fine-grained Fe (kamacite) inclusions in dusty olivines can potentially retain a primary paleomagnetic record despite significant metamorphism. For a particular magnetized grain the Neel's thermal activation theory (1) shows that the quantity

$$\frac{T\beta^{-n}\ln[\tau(T)C]}{j_s(T)h_c(T)} = \frac{v}{2k} = \text{const.} \qquad (2)$$

is constant. Particles whose relaxation times τ_r at ancient reheating temperature T_r are greater than ancient reheating time (t_r) retain the primary TRM, but grains with τ_r which is shorter than ancient reheating time are remagnetized [46]. Grains that are just on the point of being demagnetized have $\tau_r = t_r$. Thus, laboratory experiments cannot demagnetize the grains at the boundary between the primary and remagnetized populations at T_r, but only at a higher laboratory unblocking temperature T_{UB}. Because the left hand side of Eq. (2) is constant, the time–temperature relations between parameters at T_r and T_{UB} becomes

$$\frac{T_r\ln(t_rC)}{j_s(T_r)h_c(T_r)} = \frac{T_{UB}\ln(t_{lab}C)}{j_s(T_{UB})h_c(T_{UB})}. \qquad (3)$$

If we know the maximum temperature–time $(T_r - t_r)$ regime to which a rock has been exposed, a laboratory stepwise thermal demagnetization experiment and Eq. (3) tell us whether all or any of the NRM is a primary TRM or secondary remanence.

Garrick-Bethell and Weiss [47] gave reasonable approximations for the temperature dependence of $j_s(T)$ and $h_c(T)$ in Eq. (3), and presented quantitative time–temperature relations for the remagnetization of the body-centered cubic iron mineral kamacite for the first time. We employ their relations for kamacite to the thermal stability of dusty olivines in chondrules. Fig. 5 is a contour plot of $T\ln(Ct)$ for various values of the constant $j_s(T)h_c(T)$. A reliable minimum unblocking temperature is the intersection point of the horizontal line ($t = 1000$ s) and the contour passing through the estimated combination (T_r, t_r) of ancient metamorphic temperature and a maximum reheating duration [28,48,49]. Table 3 summarized maximum metamorphic temperature and reheating duration of the least metamorphosed type-3 ordinary chondrites (subtypes 3.0–3.4) and carbonaceous chondrites that frequently contain dusty olivine. The least metamorphosed type LL3.0 Semarkona meteorite indicates the maximum metamorphic temperature and its duration of

Table 3
Metamorphic temperature estimates of dusty olivine-bearing chondrites listed in Jones and Danielson [10], and their reliable unblocking temperatures estimated from the timescale of metamorphism for the maximum duration of 100 Ma [50]

Meteorite name	Type	Metamorphic temperature (°C)	Geothermometer	Estimated unblocking temperature, T_{UB} (°C)
Semarkona	LL3.0	250	Clay minerals combination [a]	490
Bishunpur	LL3.1	300–350	Ni content of matrix metals [b]	570
		~400	Ni content of phosphides in chondrule metals [b]	600
Chainpur	LL3.4	450	Noble gases abundance in diamonds [c, d]	630
Ragland	LL3.5	500–600	Order/disorder temperature of feldspar [e]	660
Murchison	CM2	~20	Oxygen isotope composition [f]	220
		87–127	Organic compounds formation [g]	350
Vigarano	CV3.3	450	Noble gases abundance in diamonds [c]	620

[a] Alexander et al. [51].
[b] Rambaldi and Wasson [20].
[c] Huss and Lewis [53].
[d] Huss et al. [54].
[e] Sears et al. [55].
[f] Clayton and Mayeda [56].
[g] Anders et al. [57].

~250 °C and 100 My [20,50,51,52]. Fig. 5 predicts that the peak metamorphic event should have demagnetized fine Fe inclusions in dusty olivines to a 1000 s unblocking temperature of 490 °C. Therefore, any magnetization observed below 490 °C in thermal demagnetization experiments of type-3 ordinary chondrites should be interpreted with caution. Only single-domain kamacite grains with unblocking temperatures greater than 490 °C should be taken as firm evidence for the retention of a primary TRM for the low-grade metamorphism of LL3.0. Fortunately, the Curie temperature of kamacite (760 °C) is much higher than these estimates, so that paleomagnetic data of dusty olivines above 490 °C is a potential source for information regarding the early solar nebula.

5. Discussion

Magnetic signatures in bulk meteorite samples result from magnetic minerals in different parts of chondrite, such as individual chondrules, shock veins and matrix (e.g., [22]). These magnetic minerals from different parts of chondrite show drastically different magnetic domain states. As a result, paleomagnetic measurements of bulk chondrite samples can be expected to reflect a highly complex averaging process, potentially leading us very far from the primary field direction and intensity. To discriminate these signatures, previous researchers extracted individual chondrules from a chondrite because it is believed that they were produced under high temperature process in early solar nebula. In ordinary chondrite of type L6 (ALHA76009), it was shown the orientations of stable remanence in each individual chondrule are scattered within the whole chondrite with no hemispherical bias and are rotated under stepwise thermal demagnetization of the remanence [58]. These paleomagnetic data suggest that each NRM was acquired as TRM under precessional motions in the presence of a nebular field before assembled into the chondrite [58]. However, it is hardly possible to preserve the original characteristics of TRM in the case of a late episode of chemical process and/or thermal metamorphism. Moreover, only paleomagnetic aspects may lead us to misinterpret the acquisition of the remanence if chondrules include secondary-formed metals in origin. Therefore, even though one can successfully extract individual chondrules from matrix, we still need to check how the stable remanence-carrying metals are formed in chondrules from their texture observations to explore the ancient nebular field. Except for barred olivine samples, our synthetic chondrules hold a remanent magnetization that is strong-field thermal remanent magnetization (TRM) in origin, because they were magnetized when they were cooled through the Curie temperature under an applied

magnetic field. Our AF demagnetization curves and BSE observations of the products indicate that samples containing dusty olivine are remarkably stable up to 80 mT, whereas porphyritic olivine samples are unstable (Fig. 2). Because AF demagnetization can be used as an estimate of a sample's coercivity, this result indicates that the dusty olivine samples have higher coercivity components than the others. Our BSE observations confirm that metallic precipitates in the dusty olivine samples are numerous fine (<1 μm) Fe inclusions embedded within the dusty olivine, and coarse (>5 μm) Fe–Ni globules located in the glassy mesostasis at the olivine grain boundaries (Fig. 4a,b). On the other hand, porphyritic olivine samples contain only coarse (>5 μm) Cr–Al-rich grains (Fig. 4d). Hence, it is likely that the presence of fine Fe inclusions results in the stable and high coercivity spectrum of dusty olivine samples, whereas the absence of fine-grained magnetic minerals is responsible for unstable behavior of porphyritic olivine. To employ a better magnetic recorder of dusty olivine-bearing chondrules, BSE observations should be made before the extraction of individual chondrules. In addition to chondrule extractions, the latest development of magnetic microscopes, such as the low-temperature superconducting SQUID microscope [59,60] or the magneto-impedance (MI) scanning microscope, [61,62] might ultimately assist efforts to read the paleomagnetic signal of sub-millimeter sized selected magnetic grains, such as dusty olivines.

Extraterrestrial chemical alteration, parent-body metamorphism and terrestrial weathering can remagnetize the primary thermal remanence in chondrules. Kohout et al. [63] suggested that the extraterrestrial magnetization could be completely remagnetized due to chemical weathering related to the presence of salt in the soil. Also, when clay minerals begin to form a progressively larger portion of whole chondrite's matrix under parent-body metamorphism or terrestrial weathering, they become potential sources for the growth of new magnetic minerals or the alteration of primary magnetic minerals with elevated temperatures in thermal demagnetization procedures or a Thellier-type paleointensity scheme [64]. In natural chondrules, the fine-grained Fe inclusions are embedded in Mg-rich host olivine [10,24]. This feature suggests that the fine Fe inclusions in dusty olivine may have been "armored" against chemical alteration by surrounding host Fe-poor olivine. Host silicates with low interstitial Fe, and hence a lower potential for the growth of magnetic minerals under low-grade metamorphic conditions, may be the best paleomagnetic targets. In our experiments, fine Fe inclusions in synthetic dusty olivines are enclosed within host Fe-poor olivine crystals (Fig. 4a,b). Furthermore, thermomagnetic measurement of one dusty olivine

sampleindicated a Curie temperature of kamacite (760 °C, Fig. 3), which indicates it is a Ni-poor (Ni < 8 wt.%) Fe–Ni alloy with body centered cubic (bcc) structure. Previous analytical transmission electron microscopic study and electron diffraction observation showed that the fine inclusions in natural dusty olivine also consist of Ni-poor (typically <2 wt.%) Fe–Ni alloy with bcc structure [25]. Therefore, we suggest that a chondrule containing dusty olivine in primitive chondrites has an ability to preserve an unaltered primary remanence. Indeed, recent paleomagnetic studies of single plagioclase crystals from Proterozoic mafic dykes found that fine-grained titanomagnetites embedded in single clear plagioclase shows very little or no oxidation, because the fine-grained titanomagnetites may have been "armored" against alteration by the plagioclase matrix in which they are embedded [39,60]. The dusty olivines in the least metamorphosed LL3.0 meteorite are likely to retain an ancient solar nebular field in stepwise thermal demagnetization experiment above 490 °C, if the host olivine crystal is not altered to clay minerals and the metal is kamacite. Therefore the fine-grained magnetic metal inclusions exsolved in silicate minerals are potentially chemically and magnetically stable tools for paleomagnetic studies [37].

The origin of remanence is an issue of the relative chronology between the reduction process and chondrule formation events. There are two possibilities to produce the dusty olivine in chondrules: (a) reduction took place during chondrule formation at high temperature, and (b) reduction took place in the chondrule precursor assemblage at low temperature. Our experimental results show that the formation of fine Fe inclusions in the synthetic dusty olivine requires heating under reducing conditions that are achieved in the presence of carbon (graphite) over several minutes. The timescale of minutes is similar to that of the flash-heating episode of chondrule formation [3]. Previous high-temperature reduction experiments of olivine also have reproduced dusty olivines on a timescale relevant for chondrule formation, using carbon as a reducing agent [8,9,25]. According to Leroux et al. [25], dusty olivine was formed by a sub-solidus reduction according to the following reaction:

$$Fe_2SiO_{4(in\ olivine)} = 2Fe_{(in\ metal)} + SiO_{2(in\ glass)} + O_{2(in\ gas)} \quad (4)$$
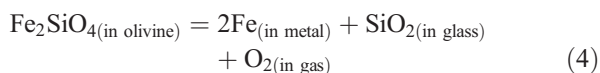
However, the metal to glass ratio observed by their analytical TEM studies has been shown to exceed the stoichiometric proportions predicted by reaction (4). They suggested that this is explained either by preferential extraction of the silica-rich melts from the olivines or by preferential volatilization of silicon monoxide. It implies

that the reaction took place at high temperatures that allow SiO_2 to exist as melt and/or vapor. Thus, our results and previous reducing experiments suggest that the fine Fe inclusions in dusty olivines were formed during chondrule formation at high temperature when carbon is present in the chondrule precursor, supporting situation (a). According to Jones and Danielson [10], the reduction could take place before chondrule formation at low temperature, perhaps by reaction of the chondrule precursor assemblage with a reducing gas, supporting situation (b). In both cases, the fine Fe inclusions would have been heated above their Curie temperature during the last chondrule forming events. Thus, we suggest that the fine Fe inclusions in dusty olivine can acquire remanent magnetization during chondrule formation events, which is expected to be a TRM in origin.

Our experiments showed that the samples containing dusty olivine hold more stable and strong remanence than the samples without dusty olivine. Since both samples were produced under similar thermal conditions (Table 1), it is clear that carbon in the form of graphite controlled the formation of the fine Fe inclusions in dusty olivine. This result implies that remanent magnetization of chondrules carried by Fe metal would be controlled by the reducing environment when they were magnetized during chondrule formation. The reducing environment that controls the occurrence of the dusty olivine could be achieved either by the reducing agents, the surrounding nebular gas, or simply by the intrinsic oxygen fugacity of a precursor assemblage that consists of metal plus forsterite. The results of the present and the previous experiments [8,25] suggest that carbon as a reducing agent in the chondrule melts is the key element that determined the reducing environment. Connolly et al. [8] and Lauretta and Buseck [65] have expounded on a chemical environment during chondrule formation in the presence of carbon. Connolly et al. [8] suggested that if carbon was incorporated into chondrule precursors, it would create a self-buffered microenvironment within and around the samples. Carbon would react with the oxygen from the samples at high temperature to produce CO gas which would be lost from the sample during their formation [8,65]. The scavenging of oxygen during carbon oxidation would result in a low oxygen fugacity, below the iron-wüstite buffer, resulting in the stabilization of metallic Fe [8]. These authors concluded that redox conditions in the chondrule were buffered by precursor minerals, particularly by carbon. If this model is correct, it is likely that the composition of the chondrule precursor materials, particularly the initial abundance of carbon, played an important role in the acquisition of remanence during chondrule formation. In the present study, we assumed that chondrule precursors were silicates

and carbon was the reducing agent. However, metal could also be incorporated into precursor assemblages. In this case, preservation of the metal should be considered. Cohen and Hewins [43] heated a CI chondrite analog material which contained troilite (FeS), kerogen, and silicates to simulate the formation of metallic iron in chondrules. They showed that Fe metal blebs which were produced mainly by the de-sulfidation of troilite survived at chondrule-forming temperatures under high total pressures (1 atm), but FeS and Fe metal were extremely volatile under lower pressures more comparable to that of the canonical nebula (1.31×10^{-5} atm). Their results imply that the pressure during chondrule formation is also important to interpretations of the acquisition process of magnetization of chondrules. Although the thermal and magnetic environment during chondrule formation is necessary to acquire TRM into magnetic minerals in chondrules, we suggest that other parameters, especially the chemical environment controlled by carbon, would also have played an important role in the acquisition of remanence during the chondrule forming processes.

6. Conclusion

Our rock magnetic study of synthetic chondrules suggests that dusty olivine-bearing chondrules are suitable for paleomagnetic studies relevant to the solar nebula, rather than barred and porphyritic chondrules without dusty olivines. The high coercivity spectrum, Curie temperature of 760 °C, theoretical time–temperature relation and BSE observations of synthetic dusty olivine indicate that fine Fe inclusions in natural dusty olivines are good carriers of a stable magnetic remanence. These inclusions may have been armored against chemical alteration by rims of clear Mg-rich olivine even in natural dusty olivines, as analogous to fine-grained titanomagnetite embedded in a terrestrial clear single plagioclase crystal. The fine Fe inclusions were heated above the Curie temperature during the last chondrule forming events, suggesting that the fine Fe inclusions in dusty olivine acquired thermal remanent magnetization during chondrule formation events. Therefore, the presence of fine-grained Fe inclusions in dusty olivine in ordinary chondrites constrains that such dusty olivine in chondrules is a good candidate for being a minimally altered and stable magnetic recorder for the early solar magnetic field.

Acknowledgments

References

[1] M.K. Weisberg, M. Prinz, Agglomeratic chondrules, chondrule precursors, and incomplete melting, in: R.H. Hewins, R.H. Jones, E.R.D. Scott (Eds.), Chondrules and the Protoplanetary Disk, Cambridge University Press, New York, 1996, pp. 119–127.

[2] J.N. Grossman, Formation of chondrules, in: J.F. Kerridge, M.S. Matthews (Eds.), Meteoritics and the Early Solar System, University of Arizona Press, Arizona, 1988, pp. 680–696.

[3] Y. Yu, R.H. Hewins, B. Zanda, Sodium and sulfur in chondrules: heating time and cooling curves, in: R.H. Hewins, R.H. Jones, E.R.D. Scott (Eds.), Chondrules and the Protoplanetary Disk, Cambridge University Press, New York, 1996, pp. 213–219.

[4] A.E. Rubin, Petrologic, geochemical and experimental constraints on models of chondrule formation, Earth-Sci. Rev. 50 (2000) 3–27.

[5] H.C. Connolly, B.D. Jones, R.H. Hewins, The flash melting of chondrules: an experimental investigation into the melting history and physical nature of chondrule precursors, Geochim. Cosmochim. Acta 62 (1998) 2725–2735.

[6] H. Nagahara, Evidence for secondary origin of chondrules, Nature 292 (1981) 135–136.

[7] E.R. Rambaldi, Relict grains in chondrules, Nature 293 (1981) 558–561.

[8] H.C. Connolly, R.H. Hewins, R.D. Ash, B. Zanda, G.E. Lofgren, M. Bourot-Denise, Carbon and the formation of reduced chondrules, Nature 371 (1994) 136–138.

[9] G. Libourel, M. Chaussidon, Experimental constrains on the origin of chondrule reduction, Meteoritics 30 (1995) 536–537.

[10] R.H. Jones, L.R. Danielson, A chondrule origin for dusty relict olivine in unequilibrated chondrites, Meteorit. Planet. Sci. 32 (1997) 753–760.

[11] L. Lamelle, F. Guyot, H. Leroux, G. Libourel, Experimental study of chemical coupling between reduction and volatilization in olivine single crystals, Geochim. Cosmochim. Acta 64 (2000) 3237–3249.

[12] S.J. Desch, T.C. Mouschovias, The magnetic decoupling stage of star formation, Astrophys. J. 550 (2001) 314–333.

[13] M. Lanoix, D.W. Strangway, G.W. Pearce, Paleointensity determinations from Allende chondrules, Lunar Planet. Sci. IX (1978) 630–632 (abstract).

[14] T. Nagata, M. Funaki, Paleointensity of the Allende carbonaceous chondrite, Proc. 8th Symp. Antarctic Meteorite, 1983, pp. 403–434.

[15] F.H. Shu, H. Shang, T. Lee, Toward an astrophysical theory of chondrites, Science 271 (1996) 1545–1552.

[16] S.J. Desch, H.C. Connolly, A model of the thermal processing of particles in solar nebula shocks: application to the cooling rates of chondrules, Meteorit. Planet. Sci. 37 (2002) 183–207.

[17] N. Sugiura, M. Lanoix, D.W. Strangway, Magnetic fields of the solar nebula as recorded in chondrules from the allende meteorite, Phys. Earth Planet. Inter. 20 (1979) 342–349.

[18] N. Sugiura, D.W. Strangway, Magnetic properties of low-petrologic grade non-carbonaceous chondrites, Mem. Natl. Inst. Polar Res., Spec. Issue 25 (1982) 260–280.

[19] S.J. Mordan, D.W. Collinson, The implications of the magnetism of ordinary chondrite meteorites, Earth Planet. Sci. Lett. 109 (1992) 185–204.

[20] E.R. Rambaldi, J.T. Wasson, Metal and associated phases in Bishunpur, a highly unequilibrated ordinary chondrite, Geochim. Cosmochim. Acta 45 (1981) 1001–1015.

[21] N. Sugiura, D.W. Strangway, Magnetic studies of meteorites, in: J.F. Kerridge, M.S. Mathews (Eds.), Meteoritics and the Early Solar System, University of Arizona Press, Arizona, 1988, pp. 595–615.

[22] D.J. Dunlop, Ö. Özdemir, Rock Magnetism: Fundamentals and Frontiers, Cambridge University Press, New York, 1997.

[23] P. Wasilewski, Magnetic characterization of the new magnetic mineral tetrataenite and its contrast with isochemical taenite, Phys. Earth Planet. Inter. 52 (1988) 150–158.

[24] E.R. Rambaldi, J.T. Wasson, Fine, nickel-poor Fe–Ni grains in the olivine of unequilibrated ordinary chondrites, Geochim. Cosmochim. Acta 46 (1982) 929–939.

[25] H. Leroux, G. Libourel, L. Lemelle, F. Guyot, Experimental study and TEM characterization of dusty olivines in chondrites: evidence for formation by in situ reduction, Meteorit. Planet. Sci. 38 (2003) 81–94.

[26] J.N. Grossman, A.E. Rubin, H. Nagahara, E.A. King, Properties of chondrules, in: J.F. Kerridge, M.S. Matthews (Eds.), Meteoritics and the Early Solar System, University of Arizona Press, Arizona, 1988, pp. 619–659.

[27] L. Néel, Some thermal aspects of rock magnetism, Adv. Phys. 4 (1955) 191–242.

[28] G. Pullaiah, E. Irving, K.L. Buchan, D.J. Dunlop, Magnetization changes caused by burial and uplift, Earth Planet. Sci. Lett. 28 (1975) 133–143.

[29] M.D. Kuz'min, Shape of temperature dependence of spontaneous magnetization of ferromagnets: quantitative analysis, Phys. Rev. Lett. 94 (2005), doi:10.1103/PhysRevLett.94.107204.

[30] R.F. Bulter, Paleomagnetism: Magnetic Domains to Geologic Terranes, Blackwell Science Inc, Oxford, 1992.

[31] M.E. Evans, M.W. McElhinny, The paleomagnetism of the Modipe gabbro, J. Geophys. Res. 71 (1966) 6053–6063.

[32] R.B. Hargraves, W.M. Young, Source of stable remanent magnetism in Lambertville diabase, Am. J. Sci. 267 (1969) 1161–1177.

[33] G.S. Murthy, M.E. Evans, D.J. Gough, Evidence of single-domain magnetite in the Michikamau anorthosite, Can. J. Earth Sci. 8 (1970) 361–370.

[34] P.R. Renne, T.C. Onstott, Laser-selective demagnetization; a new technique in paleomagnetism and rock magnetism, Science 242 (1988) 1152–1155.

[35] W. Xu, J. Ewissman, R. Van der Voo, D. Peacor, Electron microscopy of iron oxides and rock magnetic properties of banded series rocks of the Stillwater Complex, Montana, J. Geophys. Res. 102 (1997) 12139–12157.

[36] P.R. Renne, G.R. Scott, J.M.G. Glen, J.M. Feinberg, Oriented inclusions of magnetite in clinopyroxene; source of stable remanent magnetization in gabbros of the Messum Complex, Namibia, Geochem. Geophys. Geosys. 3 (2002) (article 1079), doi:10.1029/2002GC000319.

[37] J.M. Feinberg, G.R. Scitt, P.R. Renne, H.R. Wenk, Exsolved magnetite inclusions in silicates: features determining their remanence behavior, Geology 33 (2005) 513–516, doi:10.1130/G21290.1.

[38] T.S. Pick, L. Tauxe, Holocene paleointensities: Thellier experiments on submarine basaltic glass from the East Pacific Rise, J. Geophys. Res. 98 (1993) 17949–17964.

[39] J.A. Tarduno, R.D. Cottrell, A.V. Smirnov, High geomagnetic field intensity during mid-Cretaceous from Thellier analyses of single plagioclase crystals, Science 291 (2001) 1779–1783.

[40] E. Takahashi, Thermal history of lherzolite xenoliths: I. Petrology of lherzoite xenoliths from the Ichinomegata creater, Oga peninsula, northeast Japan, Geochim. Cosmochim. Acta 44 (1980) 1643–1658.

[41] H.C. Connolly, R.H. Hewins, Constraints on chondrule precursors from experimental data, in: R.H. Hewins, R.H. Jones, E.R.D. Scott (Eds.), Chondrules and the Protoplanetary Disk, Cambridge University Press, New York, 1996, pp. 129–135.

[42] J.N. Boland, A. Duba, Solid-state reduction of iron in olivine — planetary and meteoritic evolution, Nature 294 (1981) 136–139.

[43] B.A. Cohen, R.H. Hewins, An experimental study of the formation of metallic iron in chondrules, Geochim. Cosmochim. Acta 68 (2004) 1677–1689.

[44] H. Nagahara, Texture of chondrules, Mem. Natl. Inst. Polar Res., Spec. Issue 30 (1983) 61–83.

[45] U. Nitsan, Stability field of olivine with respect to oxidation and reduction, J. Geophys. Res. 79 (1974) 706–711.

[46] D.J. Dunlop, K.L. Buchan, Thermal remagnetization and the paleointensity record of metamorphic rocks, Phys. Earth Planet. Inter. 13 (1977) 325–331.

[47] I. Garrick-Bethell, B.P. Weiss, Blocking temperature relations for iron and the origins of lunar rock magnetism, Lunar Planet. Sci. XXXVII (2006) 2413 (abstract).

[48] M.F. Middleton, P.W. Schmidt, Paleothermometry of the Sydney Basin, J. Geophys. Res. 87 (1982) 5351–5359.

[49] D.J. Dunlop, Ö. Özdemir, D.A. Clark, P.W. Schmidt, Time–temperature relations for the remagnetization of pyrrhotite (Fe_7S_8) and their use in estimating paleotemperatures, Earth Planet. Sci. Lett. 176 (2000) 107–116.

[50] R. Hutchison, Meteorites: A Petrologic, Chemical and Isotopic Synthesis, Cambridge University Press, Camnrodge, 2004.

[51] C.M.O'D. Alexander, D.J. Barber, R. Hutchson, The microstructure of Semarkona and Bishunpur, Geochim. Cosmochim. Acta (1989) 3045–3057.

[52] H.Y. McSween, D.W.G. Sears, R.T. Dodd, Thermal metamorphism, in: J.F. Kerridge, M.S. Matthews (Eds.), Meteoritics and the Early Solar System, University of Arizona Press, Arizona, 1988, pp. 102–112.

[53] G.R. Huss, R.S. Lewis, Noble gases in presolar diamonds: II: Component abundances reflect thermal processing, Meteoritics 29 (1994) 811–829.

[54] G.R. Huss, G.J. MacPherson, G.J. Wasserburg, S.S. Russel, G. Srinivasan, Aluminum-26 in calcium–aluminium-rich inclusions and chondrules from unequilibrated ordinary chondrites, Meteorit. Planet. Sci. 36 (2001) 975–997.

[55] D.W.G. Sears, F.A. Hasan, J.D. Batchelor, J. Lu, Chemical and physical studies of type-3 chondrites: XI. Metamorphism, pairing, and brecciation of ordinary chondrites, Proc. Lunar Planet. Sci. 21 (1991) 493–512.

[56] R.N. Clayton, T.K. Mayeda, The oxygen isotope record in Murchison and other carbonaceous chondrites, Earth Planet. Sci. Lett. 67 (1984) 151–161.

[57] E. Anders, R. Hayatsu, M.H. Studier, Organic compounds in meteorites, Science 182 (1973) 781–790.

[58] T. Nagata, M. Funaki, The composition of natural remanent magnetization of an Antarctic chondrite, ALHA76009 (L6), Proc. Lunar Planet. Sci. Conf. 12B (1981) 1229–1241.

[59] F. Baudenbacher, N.T. Peters, J.P. Wisko, High resolution low-temperature superconductivity superconducting quantum

interference device microscope for imaging magnetic fields of samples at room temperatures, Rev. Sci. Instrum. 73 (2002) 1247–1254, doi:10.1063/1.1448142.

[60] B.P. Weiss, V. Hojatollah, F.J. Baudenbacher, J.L. Kirschvink, S.T. Stewart, D.L. Shuster, Records of an ancient Martian magnetic field in ALH84001, Earth Planet. Sci. Lett. 201 (2002) 449–463, doi:10.1016/S0012-821X(02)00728-8.

[61] M. Uehara, N. Nakamura, Microscopic magnetic field distributions of type-3 ordinary chondrites: a new magnetic microscopy, Travaux Géophysiques XXVII, 2006, p. 114, abstract.

[62] M. Uehara, N. Nakamura, Microscopic magnetic field distributions of unequilibrated ordinary chondrites, 69th Annual Meeting of the Meteoritical Society, 2006, p. 5232, abstract.

[63] T. Kohout, G. Kletetshka, M. Kobr, P. Pruner, P.J. Wasilewski, The influence of terrestrial processes on meteorite magnetic records, Phys. Chem. Earth 29 (2004) 885–897, doi:10.1016/j.pce.2004.06.004.

[64] J.A. Tarduno, R.D. Cottrell, A.V. Smirnov, The paleomagnetism of single silicate crystals: recording geomagnetic field strength during mixed polarity intervals, superchrons, and inner core growth, Rev. Geophys. 44 (2006), doi:10.1029/2005RG000189.

[65] D.S. Lauretta, P.R. Buseck, Opaque minerals in chondrules and fine-grained chondrule rims in the Bishupur (LL3.1) chondrite, Meteorit. Planet. Sci. 38 (2003) 59–79.